Available online at www.sciencedirect.com

ScienceDirect

Geochimica et Cosmochimica Acta 202 (2017) 179–189

Geochimica et Cosmochimica Acta

www.elsevier.com/locate/gca

Effect of in-stream physicochemical processes on the seasonal variations in $\delta^{13}C$ and $\delta^{18}O$ values in laminated travertine deposits in a mountain stream channel

Hao Yan, Zaihua Liu *, Hailong Sun

State Key Laboratory of Environmental Geochemistry, Institute of Geochemistry, Chinese Academy of Sciences, Guiyang 550081, China

Received 30 July 2016; accepted in revised form 20 December 2016; available online 29 December 2016

Abstract

Travertines are potential archives of continental paleoclimate. Records of stable carbon and oxygen isotopic composition ($\delta^{13}C$ and $\delta^{18}O$) in laminated travertine deposits from endogene spring waters show regular cyclic patterns which may be due to seasonal change in climate determinants such as temperature and rainfall. In this study, $\delta^{13}C$ and $\delta^{18}O$ measurements of three travertine specimens that grew naturally over the eight years, 2004–2011, at upstream, middle and downstream sites in a canal at Baishuitai, SW China, are presented. They exhibit clear seasonal variations that generally correlate with biannual laminations. Specifically, $\delta^{13}C$ and $\delta^{18}O$ values show significant positive correlation with each other for the three travertine specimens, with the correlation coefficients increasing downstream along the canal. To reveal the factors governing the seasonal and spatial variations in $\delta^{13}C$ and $\delta^{18}O$ values, newly formed travertines precipitated on Plexiglas substrates are also examined. Both $\delta^{13}C$ and $\delta^{18}O$ of the substrate travertines are low in the summer/rainy season and high in the winter/dry season, showing a great consistency with the patterns in the natural travertines. Spatially, isotope values increase downstream in both seasons, with higher increase rates in winter that are related to removal of larger fractions of dissolved inorganic carbon (DIC) from the solution and stronger kinetic isotopic fractionation in winter. Due to in-stream physicochemical processes, including $CaCO_3$ precipitation and the associated degassing of CO_2, seasonal changes in $\delta^{13}C$ and $\delta^{18}O$ in the travertines are amplified by two times between the upstream and downstream sites: this is opposite to trends for epigene (meteogene) tufas whose seasonal changes in stable isotope compositions are reduced downstream. We suggest in-stream physicochemical processes are a potential reason for underestimation of annual temperature ranges that are inferred from epigene tufa $\delta^{18}O$ data.

Keywords: Travertine; Stable isotopes; Kinetic isotopic fractionation; Paleoclimate; Baishuitai

1. INTRODUCTION

Tufa and travertine are common carbonate deposits in karst areas and seismically active areas, respectively. CO_2 degassing due to various physicochemical processes such as diffusion and utilization by aquatic plants leads to an increase of saturation with respect to $CaCO_3$ in the solution. When supersaturation reaches a threshold value, carbonate will be precipitated. The carbonates can be classified into two categories based on the origins of CO_2 in the water (Pentecost and Viles, 1994; Pentecost, 2005): (1) epigene tufa where CO_2 is sourced from the soil and atmosphere (Chafetz et al., 1991; Matsuoka et al., 2001; Andrews and Brasier, 2005; Kano et al., 2007; Kawai et al., 2009; Capezzuoli et al., 2014), and (2) endogene travertine, which forms due to multiple CO_2 sources in an endogene

* Corresponding author.
E-mail address: liuzaihua@vip.gyig.ac.cn (Z. Liu).

http://dx.doi.org/10.1016/j.gca.2016.12.031
0016-7037/

(thermogene) environment, including hydrolysis and oxidation of reduced carbon, decarbonation of limestone, or directly from the deep crust or upper mantle (Ford and Pedley, 1996; Fouke et al., 2000; Liu et al., 2003, 2010; Crossey et al., 2009). Because endogene CO_2 is generally characterized by high concentrations and enrichment in ^{13}C, endogene travertines often have higher precipitation rates and $\delta^{13}C$ values compared to epigene tufas. Both categories have been reported to record valuable paleoclimatic information (Minissale et al., 2002; Andrews and Brasier, 2005; Andrews, 2006; Liu et al., 2006; Toker et al., 2015). It has been suggested that their variations in stable carbon and oxygen isotope ($\delta^{13}C$ and $\delta^{18}O$) values and trace-element compositions reflect changes in the geochemistry of parent water or seasonal temperature/rainfall effects (Chafetz et al., 1991; Matsuoka et al., 2001; Ihlenfeld et al., 2003; Kano et al., 2004; O'Brien et al., 2006; Liu et al., 2006; Kano et al., 2007; Brasier et al., 2010; Sun and Liu, 2010). Apart from climatic factors, however, these geochemical proxies are also influenced by in-stream physicochemical processes during the travertine/tufa deposition such as evaporation and kinetic isotope effects associated with bicarbonate dehydration and rapid precipitation (Fouke et al., 2000; Andrews and Brasier, 2005; Kele et al., 2011). For instance, Wang et al. (2014) observed opposing temporal patterns of $\delta^{13}C$ and $\delta^{18}O$ values in the travertines deposited in ramp and pool environments, even under the same weather and climate conditions. This may make the interpretation of geochemical proxies in travertine/tufa quite complicated and often site-specific. To distinguish between the climatic and in-stream factors, newly formed or recent (formed within the past few decades) samples are usually investigated to interpret the meanings of geochemical proxies by comparing them with monitored instrumental data (e.g. Matsuoka et al., 2001; Sun and Liu, 2010).

Some workers (Sun and Liu, 2010; Wang et al., 2014) have used artificial substrates to collect new travertine, and monitored the physical–chemical properties of the parent water and climatic conditions at the same time. The advantage of such a method is the opportunity provided for detailed examination of the various factors controlling these geochemical proxies. Other studies (e.g. Matsuoka et al., 2001; Ihlenfeld et al., 2003; Kano et al., 2004; Liu et al., 2006; Kano et al., 2007; Hori et al., 2009; Lojen et al., 2009; Osácar et al., 2013) have also extracted climatic information from oxygen and carbon isotope and trace element profiles in recent travertine/tufa specimens. When calibrated by monitored travertine collected on artificial substrates, such recent laminated specimens can provide many years of data on the cyclic variations in oxygen and carbon isotope composition, and thus may establish the relationships between the proxies and the climatic variables not only on seasonal but also on inter-annual timescales (Matsuoka et al., 2001; Kano et al., 2007). Among the chemical indices in travertine/tufa, the use of the oxygen isotopic composition as a paleothermometer has been the principal concern in most previous studies of recent laminated samples (Kano et al., 2007). Interpretation of the carbon isotope composition in travertine/tufa is usually more complicated due to the greater variety of controlling factors (Hori et al., 2008).

In this study we present high-resolution oxygen and carbon isotope profiles of three recent travertine specimens collected in the Baishuitai canal (Yunnan, SW China), where there has been much prior work (Liu et al., 2006, 2010; Sun and Liu, 2010; Yan et al., 2012, 2016; Kele et al., 2015). One previous investigation showed that the $\delta^{13}C$ and $\delta^{18}O$ values of travertine in the canal can be used as a proxy for reconstruction of the local rainfall (Sun and Liu, 2010). Another found that the $\delta^{18}O$ values of travertine there did not reflect local temperatures but in-stream kinetic effects instead (Yan et al., 2012). The conclusions of these two studies were based on new travertine collected on artificial substrates. Thus it is of particular interest to check the mechanisms controlling stable isotopic compositions in travertine from upstream to downstream sites on a longer timescale and evaluate the effect of in-stream processes on the $\delta^{18}O$ and $\delta^{13}C$ values. We also pay attention to the differences between endogene travertine and epigene (meteogene) tufa and offer a new explanation for narrow range of annual temperature calculated from $\delta^{18}O$ data (Matsuoka et al., 2001; Brasier et al., 2010).

2. GENERAL SETTING OF THE STUDY AREA

The Baishuitai travertine site (N27°300′, E100°02′) is located ~100 km south of Shangri-La Town, Yunnan Province, China. The elevation ranges from 2380 to 3800 m asl. The area is characterized by a subtropical monsoon climate, with >75% of the annual precipitation (~750 mm) occurring during the rainy season from May to October, and an annual mean air temperature of 8 °C (Liu et al., 2003).

Intense travertine deposition takes place in an artificial canal 2.6 km in length that descends from 2900 to 2600 m asl (Fig. 1). The canal is supplied chiefly by a karst spring, S1-3, but also partially by the Baishui River during the rainy season. The spring water is a simple HCO_3–Ca hydrochemical type that reflects the dissolution of middle Triassic limestone bedrock in the catchment (Liu et al., 2010). The spring has high concentrations of Ca^{2+} and HCO_3^- and high partial pressures of CO_2, implying an endogene origin (Liu et al., 2003). The canal is small; its width ranges from 30 to 50 cm and depth from 10 to 20 cm. The flow rate ranges between 50 and 100 L/s (for more details see Sun and Liu, 2010).

3. METHODS

Three recent travertine samples were collected along the canal in January 2012 for oxygen and carbon isotope analysis. The distances from Spring S1-3 to the upstream, middle and downstream sites are about 850 m, 1500 m and 2600 m, respectively (Fig. 1). The samples each contain eight couplets of lighter and darker laminae, representing the years from 2004 to 2011 (Fig. 2). The thickness of each sample was about 12 cm, implying that the thickness of annual couplets varied from 1 to 2 cm. The samples were dried at room temperature and cut into columnar shapes.

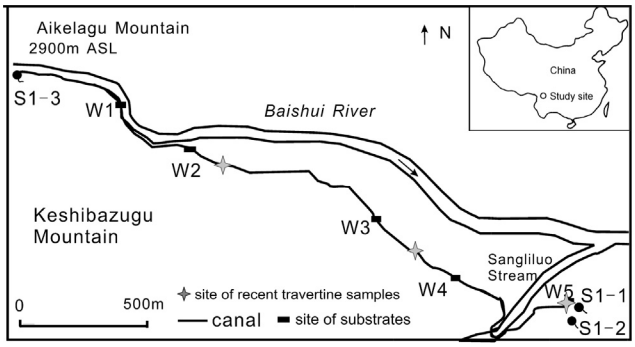

Fig. 1. Locations of the sample plexiglass substrates (solid rectangles) and the recent travertine specimens (gray stars) in the travertine-depositing canal of Baishuitai, Yunnan, SW China.

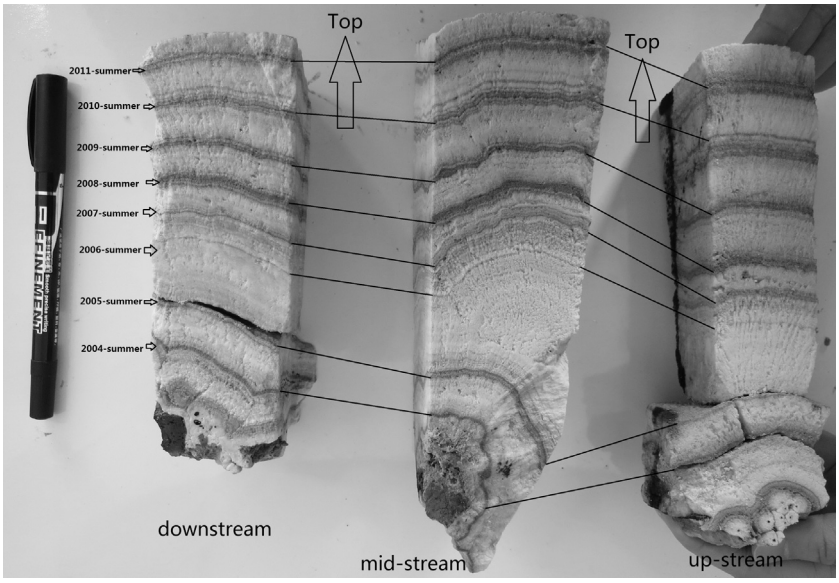

Fig. 2. The recent laminated travertine specimens (2004–2011) collected at upstream, middle and downstream sites in the Baishuitai canal, showing the regular alternation of thin darker and thick lighter layers. A couplet consisting of one thin and one thick layer is assumed to represent one annual cycle. The top outer surface corresponds to January 22, 2012, when the sample was collected.

Sub-samples were then taken using a hand dental drill at ~1 mm intervals.

In addition, new travertine samples at five sites along the canal (W1-W5) were collected on Plexiglas substrates in July, 2010 (Yan et al., 2012) and January, 2012. The substrates were immersed in stream water for ten days in summer or seven days in winter for the collection. During the sampling period, the pH, water temperature and electrical conductivity (EC) were measured *in situ* with a hand-held water quality meter (WTW 350i) with accuracies of ±0.05 pH units, ±0.1 °C and ±0.5%, respectively. The concentrations of HCO_3^- and Ca^{2+} were titrated on site via an Aquamerck® Alkalinity Test and Hardness Test with analytical resolutions of approximately ±6 and ±1 mg/L, respectively. To accurately measure solution chemistry, water samples at the sampling sites were collected in acid-cleaned polyethylene bottles and filtered through 0.45 μm Minisart® filters. A non-acidified water aliquot was used for major element concentration measurements and analysed at the State Key Laboratory of Environmental Geochemistry of the Institute of Geochemistry, Chinese Academy of Sciences. The concentrations of Na^+, K^+, and Mg^{2+} were determined via an inductively coupled plasma optical emission spectrometer (ICP-OES) with an RSD of less than 5%, and the concentrations of SO_4^{2-} and Cl^- were determined by ion chromatography (Dionex® ICS-90) with RSDs of less than 2% and 4%, respectively. The measurements of water temperature, pH and concentrations of Ca^{2+}, HCO_3^-, K^+, Na^+, Mg^{2+}, Cl^- and SO_4^{2-}, were processed with the PHREEQC program (Parkhurst and Appelo, 1999) to calculate CO_2 partial pressure (P_{CO2}) and the calcite saturation index (SI_C).

Oxygen and carbon isotopic values ($\delta^{18}O$ and $\delta^{13}C$) of sub-samples of the three recent travertine specimens and the substrate samples were measured in the State Key Laboratory of Environmental Geochemistry, Guiyang, China. For each analysis about 400 μg of travertine powder was put into a glass tube to react with 100% H_3PO_4 at 80 °C.

The generated CO_2 was then passed through a MAT 253 mass spectrometer for isotope measurements. The results were reported as ‰ vs. Vienna Pee Dee Belemnite (VPDB). The internal precision of the isotope analyses of samples was better than ±0.05‰, while the uncertainty of internal standard during entire analytical procedure was better than 0.1‰ for both $\delta^{13}C$ and $\delta^{18}O$.

4. RESULTS

Hydrochemical parameters of the stream water in the canal are presented in Table 1. All measured parameters display seasonal changes. Concentrations of Ca^{2+} and HCO_3^- ([Ca^{2+}] and [HCO_3^-]), EC, P_{CO2} and SI_C are generally higher in winter than in summer. The seasonal variations of hydrochemical properties are due to the effect of dilution by Baishui river water and overland flow in the rainy season (Liu et al., 2010). Seasonal changes in precipitation rates and in the content of clay and organic matter introduced by overland flow control the thickness and color of biannual laminations in travertine at Baishuitai (Liu et al., 2010; Yan et al., 2016).

General increases in the $\delta^{13}C$ and $\delta^{18}O$ values of substrate travertine samples are observed from upstream to downstream in the canal in both the summer and winter. However, their rates of increase differ; temporally, the winter samples being enriched in ^{13}C and ^{18}O compared to the summer samples (Fig. 3).

The $\delta^{13}C$ and $\delta^{18}O$ values of the recent travertine specimens at the upstream, middle and downstream sites in the canal are presented in Fig. 4. Generally, both $\delta^{13}C$ and $\delta^{18}O$ values show the same seasonal pattern, i.e., lower in summer and higher in winter, as observed in the newly formed travertines on the substrates. The average $\delta^{13}C$ values of travertine samples at upper, middle and lower sites are 3.7‰, 5.2‰ and 5.6‰ respectively, while for $\delta^{18}O$ the average values are −12.9‰, −12.0‰ and −11.7‰, respectively. Both the average $\delta^{13}C$ and $\delta^{18}O$ show a downstream increasing trend. The minimum and maximum values of $\delta^{13}C$ and $\delta^{18}O$ values at the three sites are given in Table 2. In addition, cross-plots of the $\delta^{13}C$ and $\delta^{18}O$ values show significant positive correlations in all the three travertine samples (Fig. 5).

5. DISCUSSION

5.1. Effects of in-channel physicochemical processes on $\delta^{13}C$ and $\delta^{18}O$ values of the travertine

5.1.1. The newly formed travertine on substrates

The isotopic data of travertine samples on substrates show that both carbon and oxygen become significantly enriched isotopically (heavier) downstream (Fig. 3). For carbon, it is well known that preferential loss of ^{12}C due to degassing of CO_2 (or HCO_3^- dehydration) is responsible for the downstream progressive increase of $\delta^{13}C$ values in the dissolved inorganic carbon (DIC) in the solution and thus in any travertine that is deposited (Usdowski et al., 1979; Dandurand et al., 1982; Sun and Liu, 2010). For oxygen, because there were no significant spatial variations of $\delta^{18}O$ in water flowing down the canal during the study period according to Yan et al. (2012), evaporative effects on oxygen isotopic composition in both water and travertine can be ignored here. Change in the temperature-dependent isotopic fractionation between travertine and water is also not the reason for spatial variations (Yan et al., 2012). Instead, downstream increase in the $\delta^{18}O$ values of the travertine may reflect the effect of HCO_3^- depletion, as reported by many cave researchers (e.g. Hendy, 1971; Dreybrodt and Scholz, 2011).

The combined fractionation factor of carbon and oxygen isotopes ($\alpha^{13}C_{total}$ and $\alpha^{18}O_{total}$) of the global reaction ($Ca^{2+} + 2HCO_3^- \rightarrow CaCO_3 + H_2O + CO_2$) can be calculated with the following equations (Dreybrodt, 2008):

$$\alpha^{13}C_{total} = \frac{1}{2}\alpha^{13}C_{CaCO_3-HCO_3} + \frac{1}{2}\alpha^{13}C_{CO_2-HCO_3} \quad (1)$$

$$\alpha^{18}O_{total} = \frac{1}{2}\alpha^{18}O_{CaCO_3-HCO_3} + \frac{1}{6}\alpha^{18}O_{H_2O-HCO_3} + \frac{1}{3}\alpha^{18}O_{CO_2-HCO_3} \quad (2)$$

where $\alpha^{13}C_{i-j}$ and $\alpha^{18}O_{i-j}$ are carbon and oxygen isotopic fractionation factors between i and j respectively. At the ambient temperature, both $\alpha^{13}C_{total}$ and $\alpha^{18}O_{total}$ are less than 1.0 due to the production of ^{13}C-depleted CO_2 and ^{18}O-depleted water. As the reaction proceeds, remaining HCO_3^- in the solution will become enriched in ^{18}O along the canal in a manner similar to carbon isotopes. However, downstream evolution of the oxygen isotopic composition is more complex because there is a huge reservoir of oxygen atoms in the water that can buffer the effect of HCO_3^- depletion (Dreybrodt, 2008; Scholz et al., 2009; Dreybrodt and Scholz, 2011). The effect of HCO_3^- depletion on $\delta^{13}C$ and $\delta^{18}O$ values of solution has been well quantified using either a classical Rayleigh-distillation model (Scholz et al., 2009) or a kinetic fractionation model (Dreybrodt, 2008). These two models are based on different assumptions and lead to different evolution of $\delta^{13}C$ and $\delta^{18}O$ values in HCO_3^-, especially where [HCO_3^-] approaches the equilibrium value. However, when the proportion of HCO_3^- removed from the solution is less than 50%, both models arrive at similar results, which can be fitted approximately by a linear Eq. (3) (Dreybrodt and Scholz, 2011).

$$\frac{R_{t\text{-}HCO3-}}{R_{0\text{-}HCO3-}} = 1 + \left(-\alpha \times \left(1 - \gamma\frac{C_{eq}}{C_0}\right) + \left(1 - \frac{C_{eq}}{C_0}\right)\right) \times \frac{t}{\tau} \quad (3)$$

where $R_{0\text{-}HCO3\text{-}}$ and $R_{t\text{-}\ HCO3\text{-}}$ are the isotopic ratios of HCO_3^- at the time when travertine begins to be deposited (R_0) and when the reaction is completed (R_t) respectively; α is the isotopic fractionation factor which can be calculated by Eqs. (1) and (2); γ is a parameter which relates $R_{0\text{-}HCO3-}$ to the isotope ratio in equilibrium ($R_{eq\text{-}HCO3-}$) ($\gamma = R_{eq\text{-}HCO3-}/R_{0\text{-}HCO3-}$) and close to 1; C_0 and C_{eq} are the initial and equilibrium concentrations of HCO_3^- respectively; t is the reaction time and τ is the time constant of precipitation for HCO_3^- (Buhmann and Dreybrodt, 1985). According to Buhmann and Dreybrodt (1985), the fraction of remaining HCO_3^- in the solution ($f = [HCO_3^-]_t/[HCO_3^-]_0$) is related to $\frac{t}{\tau}$:

Table 1
Hydrochemical compositions of stream water and stable isotopic compositions of travertine grown on substrates in the Baishuitai canal.

Site	Sampling date	Water temp.[a] (°C)	pH[a]	EC[a] (μs/cm)	K^+ (μmol/L)	Na^+ (mmol/L)	Ca^{2+}[a] (mmol/L)	Mg^{2+} (mmol/L)	Cl^- (μmol/L)	HCO_3^-[a] (mmol/L)	SO_4^{2-} (mmol/L)	pCO_2[b] (Pa)	SI_C[b]	$\delta^{13}C$ (‰)	$\delta^{18}O$ (‰)
S1-3	28-07-2010	7.9	6.94	650	16.92	0.13	3.75	0.49	n.m.	7.39	n.m.	4850	0.09	–	–
	28-01-2012	7.0	6.93	898	u.d.	0.05	5.10	0.21	12.39	9.95	0.16	6542	0.30	–	–
W1	28-07-2010	8.9	8.25	630	16.92	0.12	3.65	0.51	n.m.	7.16	n.m.	222	1.36	2.7	−12.7
	28-01-2012	6.5	8.28	853	u.d.	0.08	4.83	0.32	16.34	9.44	0.17	260	1.56	4.1	−12.4
W2	28-07-2010	9.7	8.33	615	7.69	0.10	3.55	0.43	n.m.	7.00	n.m.	180	1.43	n.m.	n.m.
	28-01-2012	6.2	8.36	820	u.d.	0.09	4.65	0.37	n.m.	9.10	n.m.	207	1.61	4.6	−12.2
W3	28-07-2010	12.2	8.43	566	8.21	0.10	3.30	0.43	n.m.	6.46	n.m.	134	1.50	3.7	−12.3
	28-01-2012	5.4	8.44	725	u.d.	0.06	4.10	0.25	10.70	8.05	0.07	153	1.58	6.2	−11.5
W4	28-07-2010	12.9	8.41	534	12.31	0.10	3.13	0.44	n.m.	6.11	n.m.	137	1.45	n.m.	n.m.
	28-01-2012	5.0	8.44	675	u.d.	0.07	3.80	0.29	n.m.	7.49	n.m.	143	1.52	7.1	−11.2
W5	28-07-2010	14.0	8.34	496	17.18	0.12	2.90	0.49	n.m.	5.70	n.m.	153	1.35	4.7	−11.9
	28-01-2012	4.7	8.39	620	1.54	0.09	3.50	0.36	4.79	6.90	0.14	150	1.40	7.9	−10.8

[a] Average values during the substrate travertine collection periods.
[b] Calculated calcite saturation index and partial pressure of CO_2 using the PHREEQC program; u.d.: under detection limit; n.m.: not measured.

$$f = \frac{[HCO_3^-]_t}{[HCO_3^-]_0} = \frac{(C_0 - C_{eq})(\exp(-\frac{t}{\tau}) - 1) + C_0}{C_0} \quad (4)$$

While f is larger than 0.6, the relationship between f and $\frac{t}{\tau}$ can approximately be expressed linearly:

$$f \approx \frac{(C_0 - C_{eq})(-\frac{t}{\tau}) + C_0}{C_0} \quad (5)$$

Replacing $\frac{t}{\tau}$ with f, Eq. (3) can be rewritten as:

$$\frac{R_{t\text{-HCO3}-}}{R_{0\text{-HCO3}-}} = 1 + (1 - f) \times \left(1 - \frac{\alpha \times (C_0 - \gamma C_{eq})}{C_0 - C_{eq}}\right) \quad (6)$$

The isotopic fractionation between travertine and HCO_3^- is:

$$\alpha_{\text{trav.}-\text{HCO3}-} = \frac{R_{trav.}}{R_{\text{HCO3}-}} \quad (7)$$

In this study, spatial changes in water temperature are never larger than 7 °C (Table 1). Within such a range of temperature, we can assume that there is no spatial variation in $\alpha_{\text{trav.}-\text{HCO3}-}$ as f decreases along the canal (O'Neil et al., 1969; Romanek et al., 1992; Beck et al., 2005). Thus, for travertine, there is:

$$\frac{R_{t-trav.}}{R_{0-trav.}} = 1 + (1 - f) \times \left(1 - \frac{\alpha \times (C_0 - \gamma C_{eq})}{C_0 - C_{eq}}\right) \quad (8)$$

In the δ-notation it can be expressed as:

$$\delta_{t-\text{trav.}} = \left[-\left(1 - \frac{\alpha \times (C_0 - \gamma C_{eq})}{C_0 - C_{eq}}\right) \times (\delta_{0-trav.} + 1000) \times f + \left(2 - \frac{\alpha \times (C_0 - \gamma C_{eq})}{C_0 - C_{eq}}\right) \times (\delta_{0-trav.} + 1000) - 1000\right] \Big/ 1000 \quad (9)$$

It is noted that Eq. (9) is only for carbon isotopes when the fraction of remaining HCO_3^- (f) is larger than 0.6. For oxygen, it is valid when the isotopic exchange rate between HCO_3^- and water is much lower than the rate of calcite precipitation so that buffering effect of bulk water can be neglected. When considering the buffering effect, $\delta^{18}O_{\text{t-trav.}}$ cannot be simply expressed as a function of f as shown in Eq. (9), though their relationship is approximately linear when $f > 0.6$.

In this study, both $\delta^{13}C$ and $\delta^{18}O$ values of the travertine correlate significantly with f as predicted by the numerical models (Fig. 6). The linear relationships in this figure follow Eqs. (10)-(13):

For summer samples:

$$\delta^{13}C_{trav.} = (-10.2 \pm 0.6) \bullet f + (12.5 \pm 0.5) \quad (R^2 = 0.996, P = 0.04, n = 3) \quad (10)$$

$$\delta^{18}O_{trav.} = (-4.2 \pm 0.0) \bullet f - (8.7 \pm 0.0) \quad (R^2 = 1, P = 0.0003, n = 3) \quad (11)$$

For winter samples:

$$\delta^{13}C_{trav.} = (-15.0 \pm 0.2) \bullet f + (18.3 \pm 0.2) \quad (R^2 = 0.999, P < 0.0001, n = 5) \quad (12)$$

$$\delta^{18}O_{trav.} = (-6.5 \pm 0.2) \bullet f - (6.3 \pm 0.2) \quad (R^2 = 0.998, P < 0.0001, n = 5) \quad (13)$$

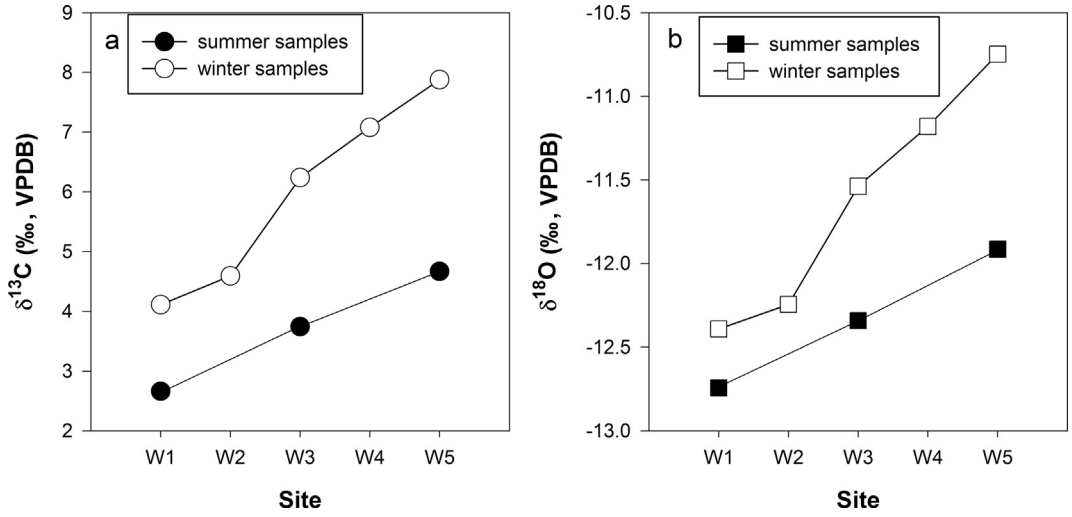

Fig. 3. Spatial and seasonal variations in (a) $\delta^{13}C$ and (b) $\delta^{18}O$ values of new travertines collected on Plexiglass substrates in the Baishuitai canal in July, 2010 and January, 2012.

For carbon, when $f = 1$ (i.e., there is no prior travertine precipitation), we obtain $\delta^{13}C_{0\text{-trav}}$ values of 2.3 ± 1.1‰ in summer from Eq. (10) and 3.3 ± 0.4‰ in winter from Eq. (12) respectively. The $\delta^{13}C_{0\text{-trav}}$ values here represent the isotopic compositions of the earliest travertine formed in the canal. These two values are very close to but slightly lower than the values measured at W1 (Table 1). This implies the location where travertine begins to be precipitated is close to W1. In addition, $\delta^{13}C_{0\text{-trav}}$ values in winter are higher than in summer, which is most likely attributed to temporal changes in carbon isotopic compositions of bicarbonate ($\delta^{13}C_{HCO3\text{-}}$). It has been particularly stated by Sun and Liu (2010) that ^{13}C-depleted river water and soil water, flowing into the canal after a rain event in summer/rainy season, could decrease $\delta^{13}C$ values of the solution and travertine precipitated from the solution. Such a so-called "isotopic dilution effect" was strong after heavy rains and weak during droughts. Sun and Liu (2010) thus suggested that the $\delta^{13}C$ values of travertine in the canal are a potential proxy for local rainfall. In this study, seasonal $\delta^{13}C_{0\text{-trav}}$ values can be reasonably interpreted by seasonal carbon isotopic compositions of the bicarbonate precipitating the earliest travertine ($\delta^{13}C_{0\text{-HCO3}-}$). Temporal variations in carbon isotopic fractionation between travertine and HCO_3^- ($\Delta^{13}C_{trav\text{-}HCO3-}$) is another potential cause to seasonal $\delta^{13}C_{0\text{-trav}}$ values. The $\delta^{13}C_{0\text{-trav}}$ value in winter would be higher with a larger $\Delta^{13}C_{trav\text{-}HCO3}$, even though the $\delta^{13}C_{0\text{-HCO3}-}$ value remains stable. For oxygen, when $f = 1$, $\delta^{18}O_0$ values of travertine in summer and winter are almost the same (-12.9 ± 0.0‰ and -12.8 ± 0.4‰ according to Eqs. (11) and (13) respectively). Compared to carbon isotope, oxygen isotope composition of water are more resistant to "isotopic dilution effect" because of a huge reservoir of oxygen atoms in bulk water. At the place where the earliest travertine is deposited (near spring vent), oxygen isotopic fractionation between travertine and water is suggested to depend mainly on water temperature (Kele et al., 2011, 2015). The narrow temperature range of spring water (Table 1) could result in a rather stable $\delta^{18}O_0$ value of travertine if $\delta^{18}O$ of water kept constant.

The slope of Eq. (9) depends on the values of α, C_{eq}, C_0 and γ. When γ is approaching to 1, the slope is dominated by the total isotopic fractionation factor (α) (Eqs. (1) and (2)). In the present study the slopes of Eqs. (12) and (13) which are fitted with winter data are steeper than those of Eqs. (10) and (11) corresponding to summer data. This implies when the same amount of HCO_3^- is removed by travertine precipitation and the associated CO_2 degassing the $\delta^{13}C$ and $\delta^{18}O$ of the travertines increase more rapidly in winter. According to Eq. (9), a smaller α value (larger isotopic fractionation because $\alpha < 1$) will lead to a steeper slope. Thus, the different slopes of Eqs. (10)-(13) imply there are stronger kinetic effects on carbon and oxygen isotopes in winter. It is reasonable as higher rates of travertine precipitation in winter are observed (Liu et al., 2010, also see thicker layer in winter in Fig. 2).For oxygen, the steeper slopes in winter may be alternatively attributed to slower exchange of oxygen isotopes between HCO_3^- and water. However, it is difficult in this study to demonstrate whether stronger kinetic fractionation or a weaker buffering effect is the dominant steepening factor.

From Eq. (9), $\delta_{t\text{-trav}}$ correlates negatively with f (Fig. 6). It is seen from Table 1 that fraction of remaining HCO_3^- in the solution at each site is higher in summer than in winter. This implies that a larger amount of HCO_3^- is removed from the solution in winter. In Table 1, $[Ca^{2+}]$, $[HCO_3^-]$, P_{CO2} and SI_C of water are all low in summer/rainy season due to dilution by rainfall (Liu et al., 2010), resulting in relatively low travertine precipitation rates (corresponding to the thin and dark layers in Fig. 2). Thus, combining a smaller f and stronger kinetic isotope fractionation, $\delta^{13}C$ and $\delta^{18}O$ of travertine increase by 3.8‰ and 1.6‰ respectively in winter, greater than the 2.0‰ and 0.8‰ in summer.

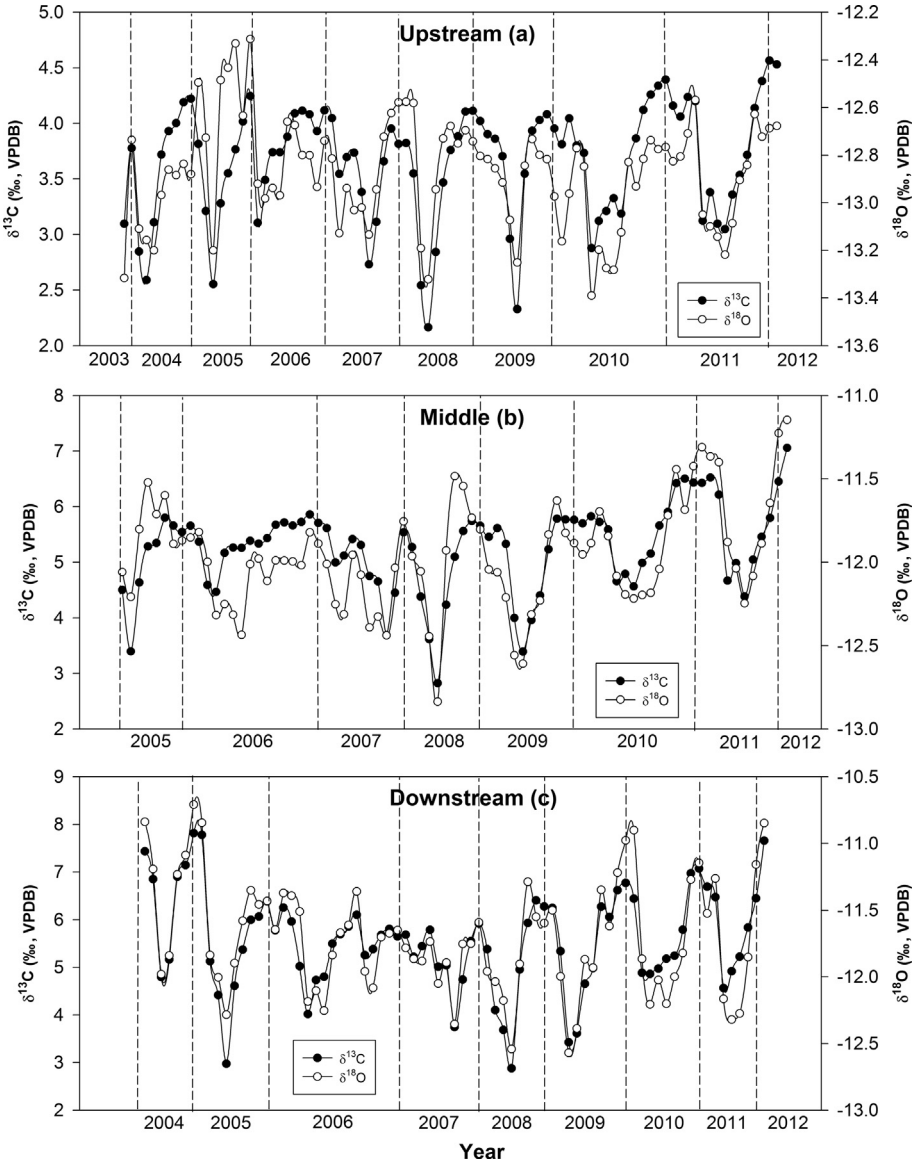

Fig. 4. Oxygen and carbon isotopic profiles from samples of three recent natural travertines in the canal. (a) upstream, (b) middle and (c) downstream location.

Overall, it is concluded that in-stream physicochemical processes can significantly increase $\delta^{13}C$ and $\delta^{18}O$ values in travertine along the canal, and that the extent of increase mainly depends on the fraction of HCO_3^- removed from the solution and the associated isotopic fractionation factor.

5.1.2. Recent travertine specimens collected at upstream, middle and downstream in the canal

Most previous studies of recent travertine and tufa have focused on the temporal variations in stable isotopic compositions and their correlation with climatic variables (Matsuoka et al., 2001; Ihlenfeld et al., 2003; Liu et al., 2006; Kano et al., 2007; Lojen et al., 2009; Osácar et al., 2013), but have paid little attention to spatial differences in the isotopic compositions of different travertine specimens along a flow path or the influence of in-stream physicochemical processes on the interpreted climatic implications (Fouke et al., 2000; Hori et al., 2009; Sürmelihindi et al., 2013). Hori et al. (2009) studied three recent tufas from different streams in SW Japan within a similar temperate climate, suggesting that the carbon isotopic composition of downstream tufa is readily affected by CO_2-degassing. When a spring water has high P_{CO2}, any change in flow rate caused by rainfall will lead to a change in the amount of CO_2 degassing and thus to a perturbation in $\delta^{13}C$ profile of the deposit (Hori et al., 2009).

In this study, the seasonal and spatial variations of $\delta^{13}C$ and $\delta^{18}O$ in the three recent travertine samples is quite consistent to those in new substrate travertines. In addition, seasonal patterns in $\delta^{13}C$ and $\delta^{18}O$ are quite clear at all three sites so that there were no unique perturbations at any one of them (Hori et al., 2009). Instead, the seasonal

Table 2
General characteristics of $\delta^{13}C$ and $\delta^{18}O$ in the three samples of natural travertine collected in the Baishuitai canal.

Sampling site	$\delta^{13}C$ (‰, VPDB)				$\delta^{18}O$ (‰, VPDB)			
	Maximum value	Minimum value	Average value	Seasonal variation	Maximum value	Minimum value	Average value	Seasonal variation
Upstream	4.6	2.2	3.7	1.5 ± 0.3	−12.3	−13.4	−12.9	0.6 ± 0.2
Middle	7.1	2.8	5.2	2.2 ± 0.5	−11.2	−12.8	−12.0	0.9 ± 0.3
Downstream	7.8	2.9	5.6	2.9 ± 0.6	−10.7	−12.6	−11.7	1.2 ± 0.3

variations in isotope composition are amplified downstream (Table 2). From up-stream to downstream sites, seasonal variations in $\delta^{13}C$ and $\delta^{18}O$ values increased by two times, from 1.5 ± 0.3‰ to 2.9 ± 0.6‰ for $\delta^{13}C$ and from 0.6 ± 0.2‰ to 1.2 ± 0.3‰ for $\delta^{18}O$.

With a record of several years of deposition, the inter-year seasonal correlations can be examined in each specimen. The $\delta^{13}C$ and $\delta^{18}O$ values of all recent travertine samples show positive correlations. Their relationship follows:

$$\text{Upstream } \delta^{18}O = (0.30 \pm 0.04) \bullet \delta^{13}C - (13.96 \pm 0.13) \times (R^2 = 0.45, P < 0.0001, n = 89) \quad (14)$$

$$\text{Middle } \delta^{18}O = (0.33 \pm 0.03) \bullet \delta^{13}C - (13.68 \pm 0.15) \times (R^2 = 0.63, P < 0.0001, n = 79) \quad (15)$$

$$\text{Downstream } \delta^{18}O = (0.37 \pm 0.02) \bullet \delta^{13}C - (13.76 \pm 0.11) \times (R^2 = 0.83, P < 0.0001, n = 77) \quad (16)$$

Two features may be noted. First, the correlation coefficients increase from upstream ($R^2 = 0.45$) to downstream site ($R^2 = 0.83$). The positive correlation between $\delta^{13}C$ and $\delta^{18}O$ values at the upstream site is mainly due to their coupled response to rainfall-related isotopic dilution effects (Sun and Liu, 2010; Wang et al., 2014). As the water flows to the downstream sites, similar evolution behaviors of the $\delta^{13}C$ and $\delta^{18}O$ values in the travertine also lead to positive correlations. Thus, the statistically more significant correlation at the downstream site can be viewed as another evidence of in-stream physicochemical processes affecting isotope signals, tending to homogenize them. Second, the slopes increase from upstream (0.30 ± 0.04) to downstream (0.37 ± 0.02), which means that a given $\delta^{13}C$ variation is related to larger $\delta^{18}O$ difference at the downstream site. This may imply that $\delta^{18}O$ values are more sensitive to in-stream physicochemical processes than to changes in the rainfall.

Sun and Liu (2010) found that the $\delta^{13}C$ and $\delta^{18}O$ values of travertine in the canal are related to local rainfall changes. Due to the in-stream physicochemical processes, the seasonal pattern of $\delta^{13}C$ and $\delta^{18}O$ are more significant at downstream sites. In Fig. 4c, there were abnormally high $\delta^{13}C$ and $\delta^{18}O$ values at downstream site at the end of 2004, 2009 and 2011, which is quite consistent with the drought history in Yunnan Province over the eight years (Yu et al., 2013). Over the severe drought there during the winter of 2009–2010 (Yang et al., 2012), the $\delta^{18}O$ anomaly seen in Fig. 4c suggests a very strong evaporation effect during that period.

It is also seen in Fig. 2 that the layers formed in 2006 are much thicker than in the other years. This is due to hydrological change after a flood on July 6, 2006 which was referred by Sun and Liu (2010) and Liu et al. (2010). Before the flood, the canal was fed by both groundwater and Baishui River water which is characterized by low $[Ca^{2+}]$ and $[HCO_3^-]$. On July 7, 2006, however, the connecting path between the canal and Baishui River was destroyed by the flood, and then the canal was only supplied by groundwater. Due to lack of dilution effect by surface water in 2006, more travertines were deposited. The hydrological change was also recorded by isotopic compositions in

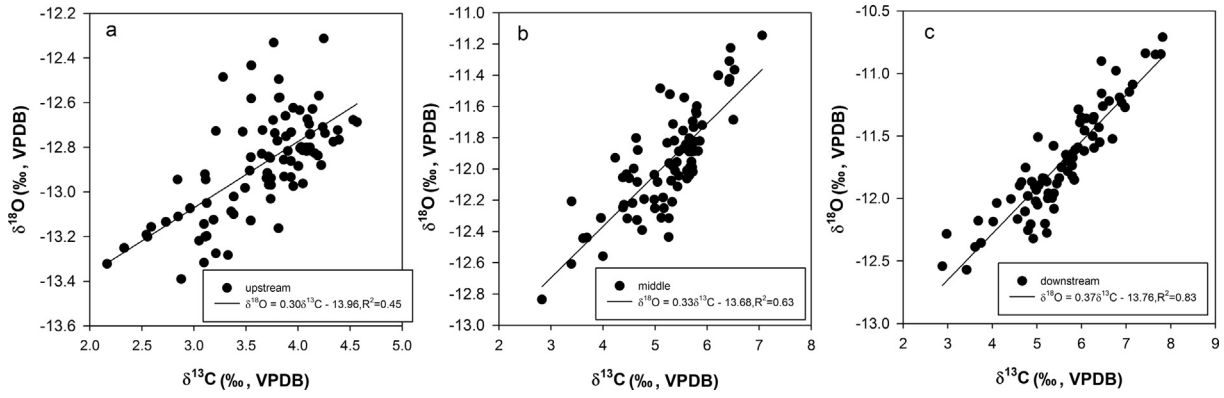

Fig. 5. Cross-plots of $\delta^{13}C$ and $\delta^{18}O$ values of the natural travertine specimens from the Baishuitai canal.

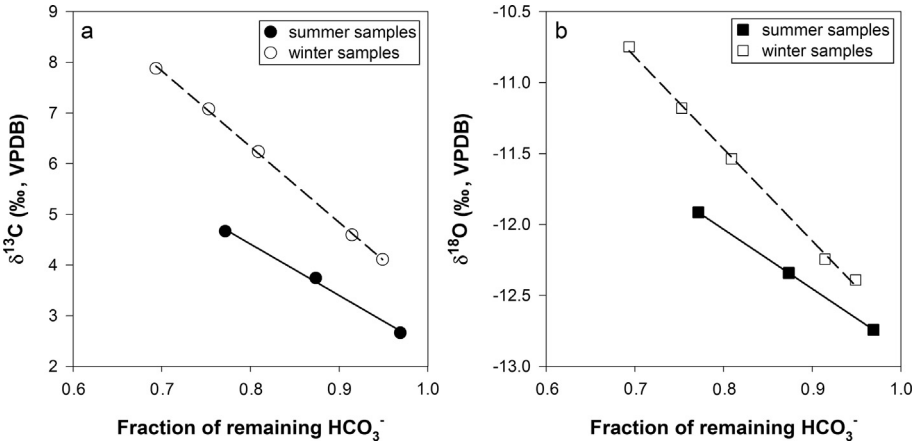

Fig. 6. Negative correlations between (a) $\delta^{13}C$ and (b) $\delta^{18}O$ of the substrate travertines and the fraction of remaining HCO_3^- in the solution in the canal.

recent travertines. The travertines formed in 2006 have narrow seasonal ranges of $\delta^{13}C$ and $\delta^{18}O$ values when compared with other years (Fig. 4), which implies a relatively stable geochemistry of water after hydrological change. In addition, isotopic compositions, especially for carbon, were generally heavier in 2006 than in other years, reflecting a weaker "isotopic dilution effect" during that period.

5.2. Comparison with epigene tufa-depositing systems

The effect of in-stream physicochemical processes on the isotopic composition of epigene tufa has been described by Hori et al. (2009). These authors observed that seasonal variation in $\delta^{13}C$ values in groundwater become reduced in the downstream travertines, especially where a spring water has high P_{CO2}. This is the opposite of the findings in this study. Comparing the two depositing systems, there are similar seasonal patterns in $\delta^{13}C$ and $\delta^{18}O$ values in the travertine/tufa (i.e., low in summer and high in winter). However, concentrations of HCO_3^-, P_{CO2} and SI_C in epigene tufa-depositing streams are high in summer–autumn (June–October) and low in winter–spring (November–May), owing to the changes in soil CO_2 productivity and ventilation (Hori et al., 2008, 2009). Precipitation rates for tufa are high in summer–autumn and low in winter–spring (Kano et al., 2003) and the amount of CO_2 degassing follows a similar seasonal variation. When CO_2 out-gassing is intense in summer, low $\delta^{13}C$ in spring water will be counteracted at downstream sites, leading to significant perturbations in the tufa $\delta^{13}C$ profiles. Comparing Hori et al.'s data with ours, we can readily determine whether amplified or reduced seasonal changes in isotopic compositions of the travertine/tufa profile depend on the seasonal relationships between isotopic composition and $CaCO_3$ precipitation rates. Where high $\delta^{13}C$ and $\delta^{18}O$ values in endogene headwaters coincide with high precipitation rates, the greater amount of HCO_3^- will be removed from the solution and consequently amplify the seasonal changes (as shown in this study), whereas the opposite will be observed in epigene waters (Hori et al., 2009).

Many studies of epigene tufas have shown that seasonal temperature variations calculated from tufa $\delta^{18}O$ values are much smaller than the actual measured temperature ranges (Chafetz et al., 1991; Matsuoka et al., 2001; Ihlenfeld et al., 2003; O'Brien et al., 2006; Brasier et al., 2010). Matsuoka et al. (2001) attributed this mismatch to the irregularity of tufa surfaces. They suggested that the $\delta^{18}O$ value of each sub-specimen corresponds to several months of deposition and thus records an average temperature for that period. Brasier et al. (2010) found that discontinuous deposition

may be responsible for the mismatch. Based on petrographic examinations, they suggested that there are no precipitates in mid-summer and mid-winter, thus $\delta^{18}O$ values record only the temperature variation during spring and autumn. Based on the data in our study, we propose an alternative explanation. In the tufa-depositing system, CO_2 in the groundwater mainly derives from soil CO_2. Thus P_{CO2} and $[HCO_3^-]$ of groundwater is generally higher in summer than in winter. With higher $[HCO_3^-]$ and temperature, the rates of precipitation of tufa are also higher in summer. Thus, greater amounts of HCO_3^- are being removed before the water reached the tufa-collecting site. This implies a smaller f value in Eq. (9) and thus a larger increase in $\delta^{18}O_{HCO3-}$ and $\delta^{18}O_{tufa}$ in summer. The effect of the temperature-dependence of oxygen isotope fractionation is partly counteracted by the effect of these in-stream physicochemical processes, resulting in a narrower range of $\delta^{18}O$ variation. Thus, we suggest, for epigene tufa, in-stream carbonate precipitation and the associated CO_2 degassing may be a potential reason for underestimation of annual temperature range inferred from $\delta^{18}O$ data.

6. CONCLUSIONS

Active travertines collected on Plexiglas substrates and three samples of recent natural travertine deposited along a canal at Baishuitai, Yunnan Province (SW China) were analysed to study the temporal and spatial variations in oxygen and carbon isotopic compositions and their controlling factors. Both $\delta^{13}C$ and $\delta^{18}O$ values of travertine show downstream increase in summer and winter, with a larger increase in winter. This is because more HCO_3^- is removed from the solution, combined with stronger kinetic isotope fractionations. It was also found that $\delta^{18}O$ and $\delta^{13}C$ values of travertine are lower in summer and higher in winter, showing positive correlation with each other. In addition, seasonal variations in $\delta^{13}C$ and $\delta^{18}O$ in the travertine that originate from rainfall changes are amplified approximately two times at a downstream site due to in-stream physicochemical processes. In contrast, for meteogene (epigene) tufa, because high deposition rates often occur in summer when $\delta^{13}C$ and $\delta^{18}O$ values are low, in-stream physicochemical processes including carbonate precipitation and bicarbonate dehydration reduce the seasonal variations in $\delta^{13}C$ and $\delta^{18}O$ values. Seasonal temperature changes may therefore be underestimated by tufa $\delta^{18}O$ data.

ACKNOWLEDGEMENTS

This study was supported by the National Natural Science Foundation of China (Grant Nos. 41172232, 41372263, and U1301231). Special thanks are given to Derek Ford and Sándor Kele and anonymous reviewers for their thoughtful comments and suggestions, which greatly improved the original draft.

REFERENCES

Andrews J. E. (2006) Palaeoclimatic records from stable isotopes in riverine tufas: synthesis and review. *Earth Sci. Rev.* **75**, 85–104.

Andrews J. E. and Brasier A. T. (2005) Seasonal records of climatic change in annually laminated tufas: short review and future prospects. *J. Quat. Sci.* **20**, 411–421.

Beck W. C., Ethan L., Grossman E. L. and Morse J. W. (2005) Experimental studies of oxygen isotope fractionation in the carbonic acid system at 15 °C, 25 °C, and 40 °C. *Geochim. Cosmochim. Acta* **69**, 3493–3503.

Brasier A. T., Andrews J. E., Marca-Bell A. D. and Dennis P. F. (2010) Depositional continuity of seasonally laminated tufas: implications for $\delta^{18}O$ based palaeotemperatures. *Global Planet. Change* **71**, 160–167.

Buhmann D. and Dreybrodt W. (1985) The kinetics of calcite dissolution and precipitation in geologically relevant situations of karst areas: 1. Open system. *Chem. Geol.* **48**, 189–211.

Capezzuoli E., Gandin A. and Pedley M. (2014) Decoding tufa and travertine (fresh water carbonates) in the sedimentary record: the state of the art. *Sedimentology* **61**, 1–21.

Chafetz H. S., Utech N. M. and Fitzmaurice S. P. (1991) Differences in the $\delta^{18}O$ and $\delta^{13}C$ signatures of seasonal laminae comprising travertine stromatolites. *J. Sediment. Res.* **61**, 1015–1028.

Crossey L. J., Karlstrom K. E., Springer A. E., Newell D., Hilton D. R. and Fischer T. (2009) Degassing of mantle-derived CO_2 and He from springs in the southern Colorado Plateau region—Neotectonic connections and implications for groundwater systems. *Geol. Soc. Am. Bull.* **121**, 1034–1053.

Dandurand J. L., Gout R., Hoefs J., Menschel G., Schott J. and Usdowski E. (1982) Kinetically controlled variations of major components and carbon and oxygen isotopes in a calcite-precipitating spring. *Chem. Geol.* **36**(3–4), 299–315.

Dreybrodt W. (2008) Evolution of the isotopic composition of carbon and oxygen in a calcite precipitating H_2O–CO_2–$CaCO_3$ solution and the related isotopic composition of calcite instalagmites. *Geochim. Cosmochim. Acta* **72**, 4712–4724.

Dreybrodt W. and Scholz D. (2011) Climatic dependence of stable carbon and oxygen isotope signals recorded in speleothems: from soil water to speleothem calcite. *Geochim. Cosmochim. Acta* **75**, 734–752.

Ford T. D. and Pedley H. M. (1996) A review of tufa and travertine deposits of the world. *Earth Sci. Rev.* **41**, 117–175.

Fouke B. W., Farmer J. D., Des Marais D. J., Pratt L., Sturchio N. C., Burns P. C. and Discipulo M. K. (2000) Depositional facies and aqueous-solid geochemistry of travertine depositing hot springs (Angel Terrace, Mammoth Hot Springs, Yellowstone National Park, U.S.A). *J. Sediment. Res.* **70**, 565–585.

Hendy C. H. (1971) The isotopic geochemistry of speleothems: I. The calculation of effects of different modes of formation on the isotopic composition of speleothems and their applicability as paleoclimatic indicators. *Geochim. Cosmochim. Acta* **35**, 801–824.

Hori M., Hoshino K., Okumura K. and Kano A. (2008) Seasonal patterns of carbon chemistry and isotopes in tufa depositing groundwaters of southwestern Japan. *Geochim. Cosmochim. Acta* **72**, 480–492.

Hori M., Kawai T., Matsuoka J. and Kano A. (2009) Intra-annual perturbations of stable isotopes in tufas: effects of hydrological processes. *Geochim. Cosmochim. Acta* **73**, 1684–1695.

Ihlenfeld C., Norman M. D., Gagan M. K., Drysdale R. N., Maas R. and Webb J. (2003) Climatic significance of seasonal trace element and stable isotope variations in a modern freshwater tufa. *Geochim. Cosmochim. Acta* **67**, 2341–2357.

Kano A., Matsuoka J., Kojo T. and Fujii H. (2003) Origin of annual laminations in tufa deposits, southwest Japan. *Palaeogeogr. Palaeoclimatol. Palaeoecol.* **191**, 243–262.

Kano A., Kawai T., Matsuoka J. and Ihara T. (2004) High-resolution records of rainfall event from clay bands in tufa. *Geology* **32**, 793–796.

Kano A., Hagiwara R., Kawai T., Hori M. and Matsuoka J. (2007) Climatic conditions and hydrological change recorded in a high-resolution stable-isotope profile of a recent laminated tufa on a subtropical island, southern Japan. *J. Sediment. Res.* **77**, 59–67.

Kawai T., Kano A. and Hori M. (2009) Geochemical and hydrological controls on biannual lamination of tufa deposits. *Sediment. Geol.* **213**, 41–50.

Kele S., Özkul M., Fórizs I., Gökgöz A., Baykara M. O., Alçiçek M. C. and Németh T. (2011) Stable isotope geochemical study of Pamukkale travertines: new evidences of low-temperature non-equilibrium calcite-water fractionation. *Sediment. Geol.* **238**, 191–212.

Kele S., Breitenbach S. F. M., Capezzuoli E., Meckler A. N., Ziegler M., Millan I. M., Kluge T., Deák J., Hanselmann K., John C. M., Yan H., Liu Z. and Bernasconi S. M. (2015) Temperature dependence of oxygen- and clumped isotope fractionation in carbonates: a study of travertines and tufas in the 6–95 °C temperature range. *Geochim. Cosmochim. Acta* **168**, 172–192.

Liu Z., Zhang M., Li Q. and You S. (2003) Hydrochemical and isotope characteristic of spring water and travertine in the Baishuitai area (SW China) and their meaning for paleoenvironmental reconstruction. *Environ. Geol.* **44**, 698–704.

Liu Z., Li H., You C., Wan N. and Sun H. (2006) Thickness and stable isotopic characteristics of modern seasonal climate-controlled sub-annual travertine laminas in a travertine-depositing stream at Baishuitai, SW China: implications for paleo-climate reconstruction. *Environ. Geol.* **51**, 257–265.

Liu Z., Sun H., Lu B., Liu X., Ye W. and Zeng C. (2010) Wet-dry seasonal variations of hydrochemistry and carbonate precipitation rates in a travertine-depositing canal at Baishuitai, Yunnan, SW China: implications for the formation of biannual laminae in travertine and for climatic reconstruction. *Chem. Geol.* **273**, 258–266.

Lojen S., Trkov A., Ščančar J., Vázquez-Navarro J. A. and Cukrov N. (2009) Continuous 60-year stable isotopic and earth-alkali element records in a modern laminated tufa (Jaruga, river Krka, Croatia): Implications for climate reconstruction. *Chem. Geol.* **258**, 242–250.

Matsuoka J., Kano A., Oba T., Watanabe T., Sakai S. and Seto K. (2001) Seasonal variation of stable isotopic compositions recorded in a laminated tufa, SW Japan. *Earth Planet. Sci. Lett.* **192**, 31–44.

Minissale A., Kerrick D. M., Magro G., Murrell M. T., Paladini M., Rihs S., Sturchio N. C., Tassi F. and Vaselli O. (2002) Geochemistry of Quaternary travertines in the region north of Rome (Italy): structural, hydrologic and paleoclimatic implications. *Earth Planet. Sci. Lett.* **203**, 709–728.

O'Brien G. R., Kaufman D. S., Sharp W. D., Atudorei V., Parnell R. A. and Crossey L. J. (2006) Oxygen isotope composition of annually banded modern and mid-Holocene travertine and evidence of paleomonsoon floods, Grand Canyon, Arizona, USA. *Quaternary Res.* **65**, 366–379.

O'Neil J., Clayton R. and Mayeda T. (1969) Oxygen isotope fractionation in divalent metal carbonates. *J. Chem. Phys.* **51**, 5547–5558.

Osácar M. C., Arenas C., Vázquez-Urbez M., Sancho C., Auqué L. F. and Pardo G. (2013) Environmental factors controlling the $\delta^{13}C$ and $\delta^{18}O$ variations of recent fluvial tufas: a 12-year record from the Monasterio de Piedra Natural Park (Ne Iberian Peninsula). *J. Sediment. Res.* **83**, 309–322.

Parkhurst D. L. and Appelo C. A. J. (1999) User's guide to PHREEQC-a computer program for speciation, batch-reaction, one-dimensional transport, and inverse geochemical calculations. *U.S. Geol. Surv. Water Resour. Invest.*, 99–4259.

Pentecost A. (2005) *Travertine*. Springer Science & Business Media.

Pentecost A. and Viles H. (1994) A review and reassessment of travertine classification. *Géog. Phys. Quatern.* **48**, 305–314.

Romanek C. S., Grossman E. L. and Morse J. W. (1992) Carbon isotopic formation in synthetic aragonite and calcite: effects of temperature and precipitation rate. *Geochim. Cosmochim. Acta* **56**, 419–430.

Scholz D., Mühlinghaus C. and Mangini A. (2009) Modelling $\delta^{13}C$ and $\delta^{18}O$ in the solution layer on stalagmite surfaces. *Geochim. Cosmochim. Acta* **73**, 2592–2602.

Sürmelihindi G., Passchier C. W., Baykan O. N., Spötl C. and Kessener P. (2013) Environmental and depositional controls on laminated freshwater carbonates: an example from the Roman aqueduct of Patara, Turkey. *Palaeogeogr. Palaeoclimatol. Palaeoecol.* **386**, 321–335.

Sun H. and Liu Z. (2010) Wet–dry seasonal and spatial variations in the $\delta^{13}C$ and $\delta^{18}O$ values of the modern endogenic travertine at Baishuitai, Yunnan, SW China and their paleoclimatic and paleoenvironmental implications. *Geochim. Cosmochim. Acta* **74**, 1016–1029.

Toker E., Kayseri-Özer M. S., Özkul M. and Kele S. (2015) Depositional system and palaeoclimatic interpretations of Middle to Late Pleistocene travertines: Kocabaş, Denizli, south-west Turkey. *Sedimentology* **62**, 1360–1383.

Usdowski E., Hoefs J. and Menschel G. (1979) Relationship between ^{13}C and ^{18}O fractionation and changes in major element composition in a recent calcite-depositing spring—A model of chemical variations with inorganic $CaCO_3$ precipitation. *Earth Planet. Sci. Lett.* **42**(2), 267–276.

Wang H., Yan H. and Liu Z. (2014) Contrasts in variations of the carbon and oxygen isotopic composition of travertines formed in pools and a ramp stream at Huanglong Ravine, China: implications for paleoclimatic interpretations. *Geochim. Cosmochim. Acta* **125**, 34–48.

Yan H., Sun H. and Liu Z. (2012) Equilibrium vs. kinetic fractionation of oxygen isotopes in the two low-temperature travertine-depositing systems with distinct hydrodynamic conditions at Baishuitai, Yunnan SW China. *Geochim. Cosmochim. Acta* **95**, 63–78.

Yang H., Song J., Yan H. M. and Li C. (2012) Cause of the severe drought in Yunnan Province during winter of 2009 to 2010. *Clim. Environ. Res.* **17**(3), 315–326 (in Chinese).

Yan H., Schmitt A., Liu Z., Sophie G., Sun H., Chen J. and Chabaux F. (2016) Calcium isotopic fractionation during travertine deposition under different hydrodynamic conditions at Baishuitai (Yunnan, SW China). *Chem. Geol.* **426**, 60–70.

Yu W., Shao M., Ren M., Zhou H., Jiang Z. and Li D. (2013) Analysis on spatial and temporal characteristics drought of Yunnan Province. *Acta Ecol. Sin.* **33**(6), 317–324.

Associate editor: F. McDermott